AMTC Letters
Vol. 1 (2008)

# Nanostructural characterization of initial crystallization of silicon carbide on 6H-SiC by solution growth method

Takeharu Kato[1)], Yoshihiro Sugawara[1)], Tsukasa Hirayama[1)], Yuichi Ikuhara[1)], Yoshitomo Shintani[2)], Hidemitsu Sakamoto[2)], Yoichiro Kawai[2)]

[1)]Nano Structures Research Laboratory, Japan Fine Ceramics Center, 2-4-6 Mutsuno Atsuta-ku, Nagoya, 456-8587, Japan

[2)]Material Engineering Div. 3, Vehicle Engineering Group, Higashifuji Technical Center, Toyota Motor Corporation,1200, Mishuku, Susono, Shizuoka, 410-1193, Japan

High-quality silicon carbide (SiC) is being developed for superior semiconductor devices with a wide-gap. Sublimation method is major technique to produce high-quality SiC crystal. Recently solution growth method has been paid an attention to produce single crystal of SiC because of not only high quality but also high growth rate. However, the growth mechanism of SiC layer, generation or disappearance of defects in the SiC are still unclear. In this study, we characterized the nanostructures of grown SiC layer formed on 6H-SiC seed by solution growth method, using transmission electron microscopy (TEM).

6H-SiC seed with a (0001) basal-plane orientation was dipped in Si-C solution containing Al. Then, the seed was pulled up immediately. A focused-ion-beam (FIB) microsampling technique was employed to prepare a cross-sectional TEM specimen of the interface between the grown SiC and the 6H-SiC seed. Hitachi FB2100 with accelerating voltage at 10-40keV was used as FIB system. Nanostructural characterization of the specimen was performed by TOPCON-EM 002B operated at accelerating voltage of 200keV.

Figure 1(a) shows a cross-sectional TEM image of the grown SiC layer/the 6H-SiC seed and (a')-(d') selected area diffraction patterns (SADP) corresponding to the regions A-D in Fig. 1(a). Incident direction of electron beam of SADP (a')-(d') is parallel to the $[\bar{1}\bar{1}20]$ of 6H-SiC, the $[0\bar{1}1]$ of 3C-SiC, both of the $[\bar{1}\bar{1}20]$ of 6H-SiC and the $[0\bar{1}1]$ of 3C-SiC, and the $[\bar{1}\bar{1}20]$ of 6H-SiC, respectively. According to these SADPs, the grown SiC layer is composed of 6H-SiC and 3C-SiC. The orientation relationship between 6H-SiC and 3C-SiC is as follows; $(0001)[\bar{1}\bar{1}20]_{\text{6H-SiC}}//(111)[0\bar{1}1]_{\text{3C-SiC}}$.

Figure 2 shows dark field images of the interface (a) under the $\vec{g} = 0006$ of 6H-SiC condition (b) under the $\vec{g} = \bar{1}100$ of 6H-SiC condition. Incident electron beam was parallel to the interface between the grown SiC and the seed under the $\vec{g} = 0006$ condition. Numbers of stacking faults are observed in the grown SiC, in addition, defects density at the vicinity of the interface is much higher than that of other grown SiC regions. Although some edge dislocations are generated from the stacking faults parallel to the basal plane of 6H-SiC, the stacking faults prevent growth of these dislocations, as shown in Fig. 2(b). Furthermore, EDS analyses indicated high Al contents in the grown SiC at the vicinity of the interface. Since the high Al content reduce the stacking fault energy of the grown SiC, the high density of the stacking faults and other defects are presumably formed in the grown SiC.

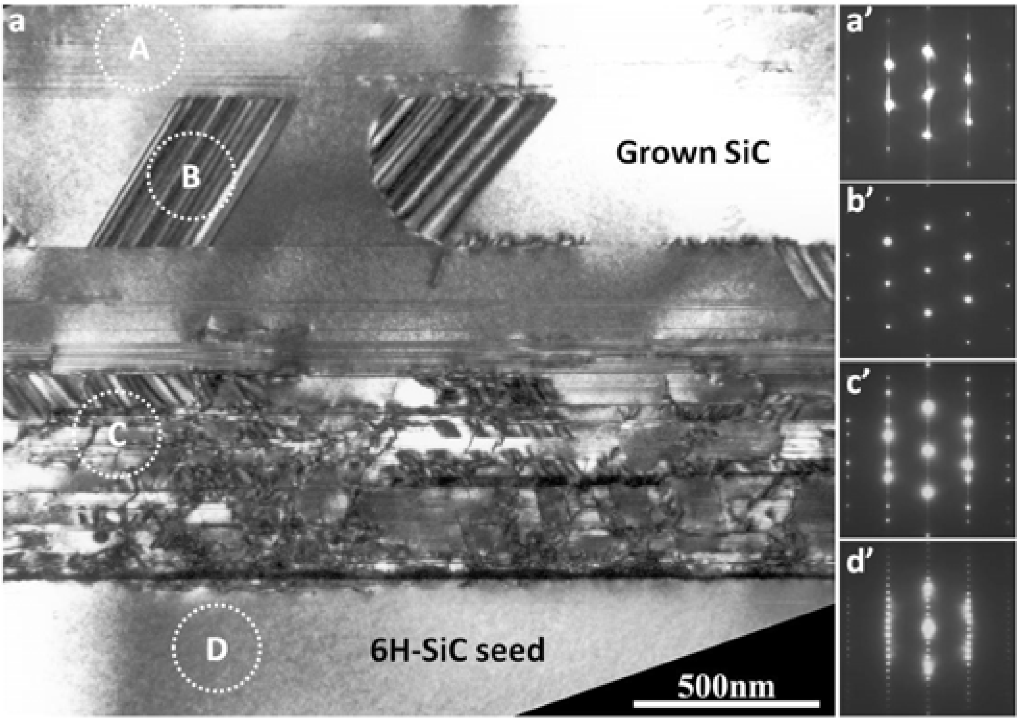

Fig. 1(a) A cross-sectional TEM image of the grown SiC layer/6H-SiC seed and (a')-(d') SADPs corresponding to the regions A-D (a).

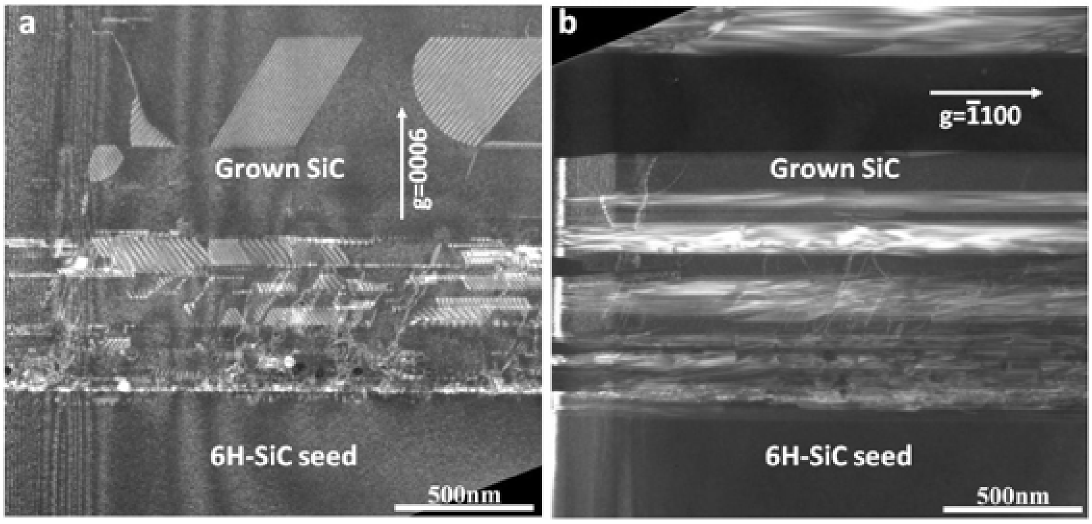

Fig. 2 Dark-field TEM images of the interface (a) under the $\vec{g} = 0006$ of 6H-SiC condition (b) under the $\vec{g} = \bar{1}100$ of 6H-SiC condition.